Smart Structures and Systems, *Vol. 34, No. 6 (2024) 415-429*
https://doi.org/10.12989/sss.2024.34.6.415

ResNet transfer learning for accurate and efficient anomaly detection of bridge vibration data

Jianxiao Mao [1a], Xun Su[*1], Gui Gui [1], Hao Wang[**1], Yuguang Fu [2] and Dan Li [1]

[1] *Key laboratory of Concrete and Prestressed Concrete Structures of Ministry of Education, Southeast University, Nanjing 211189, China*
[2] *School of Civil and Environmental Engineering, Nanyang Technological University, 639798, Singapore*

(*Received February 21, 2024, Revised December 16, 2024, Accepted January 5, 2025*)

Abstract. Dynamic properties extracted from bridge acceleration responses are critical for assessing safety, particularly in the context of long-span cable-supported bridges with main spans exceeding one kilometer. However, the abundance of acceleration sensors in their Structural Health Monitoring (SHM) systems is compromised by frequent failures in harsh operational environments, leading to significant issues of missing or erroneous vibration monitoring data. Recent advancements in deep learning offer promising solutions to diagnose the monitored abnormal bridge vibration data. Existing methods often rely on single-bridge vibration monitoring data, posing challenges in applying models across different bridges. To address these challenges, this study proposes a novel ResNet-based feature extraction method for bridge vibration data anomaly detection, emphasizing time-efficient classification and transfer learning. The timeseries bridge vibration responses are transformed into images to enhance computation efficiency. The proposed methodology leverages a pre-trained ResNet50 network for feature extraction, feeding extracted feature vectors into a k-means clustering algorithm for classification. Transfer learning with labelled training datasets ensures detection performance across different bridges, minimizing the required training data. Validation utilizes long-term vibration monitoring data from the SHM system of Sutong Bridge. The results aim to provide reliable technical support for data-driven condition assessment and maintenance of long-span bridges, addressing challenges in SHM systems and contributing to the safety and sustainability of critical infrastructure.

Keywords: anomaly detection; long-span bridges; ResNet transfer learning; structural health monitoring; vibration data

1. Introduction

The long-span bridges are usually equipped with enormous sensors to measure static and dynamic responses at both the global and local structural levels, for the evaluation of their health condition during their service life, thus achieving timely maintenance and management (Wong 2007, Catbas *et al*. 2008, Yarnold and Moon 2015). In recent years, the rapid development of digital and intelligent technologies, combined with abundant monitoring data and bridge digital twin models, has significantly improved the accuracy of sensing and dynamic modeling of bridge service conditions. The governments of many countries introduced some policies to install or upgrade structural health monitoring (SHM) system for long-span bridges to ensure their operation safety (Memisoglu *et al*. 2022, Figueired and Brownjohn 2022, Su *et al*. 2025). Existing research has indicated that bridge SHM system often records erroneous data, which can influence health assessments and cause significant analysis deviations (Annamdas *et al*. 2017, Zhou *et al*. 2020, Sun *et al*. 2020, Ni *et al*. 2020, Entezami *et al*. 2023, Xu *et al*. 2024). Therefore, ensuring the authenticity and effectiveness of the data recorded by the bridge SHM system is a fundamental prerequisite and foundation for achieving the abovementioned objectives.

The dynamic properties extracted from the bridge acceleration responses are crucial indicators for assessing structural safety and sustainability. They constitute an essential aspect of structural health monitoring for long-span bridges. For cable-supported bridges with main span exceeding one kilometer, the proportion and quantity of acceleration sensors recorded by their SHM system are relatively high (Mao *et al*. 2021). However, due to the harsh operational environment, intermittent and permanent failures of acceleration sensors frequently occurred. This leads to a significant issue of missing or erroneous vibration monitoring data, necessitating urgent research into efficient identifying and recovering methods. In recent years, deep learning methods have gradually been applied to diagnosis of the abnormal bridge monitoring data (Fu *et al*. 2019, Zhang *et al*. 2022, Ye *et al*. 2023). For instance, Bao *et al*. (2018) utilized long-term records of vibration monitoring data from bridge SHM system to generate acceleration time history graphs with a one-hour data time length, and then combined deep neural networks for data anomaly detection. They later inputted the spectral graphs alongside the time history graphs into convolutional neural networks for diagnosis (Zhang and Yuen 2021) proposed an online

*Corresponding author, Ph.D.,
E-mail: 230228341@seu.edu.cn
**Co-corresponding author, Ph.D., Professor,
E-mail: wanghao1980@seu.edu.cn
[a] Ph.D., E-mail: jianxiao@seu.edu.cn

Copyright © 2024 Techno-Press, Ltd.

ISSN: 1738-1584 (Print), 1738-1991 (Online)

approach for detecting anomalies of the structural health monitoring data based on the Bayesian dynamic linear model. They demonstrated that the proposed approach exhibits good accuracy and high computational efficiency and allows for reconstructing the strain measurements to replace anomalies. Ye *et al*. (2023) utilized wavelet scale maps to transform acceleration data into three-channel images, subsequently employing the GoogLeNet image classification neural network for diagnosing the abnormal data. Du *et al*. (2022) simultaneously utilized the time-domain and frequency-domain data images as the input of deep neural networks for diagnosing the abnormal SHM data. Chou *et al*. (2022) compared various deep learning approaches for anomaly data classification and proposed an ensemble neural network model to achieve the best performance. Recently, Mondal *et al*. (2023) developed an edge intelligence framework for the on-board deep learning computing of data anomaly classification, facilitating quality enhancement of acquired data before transmitting to a central system, in which network compression techniques can reduce the deep learning model size by 97% while still achieving the accuracy of 94.5%. Progress has been made in the diagnosis of bridge vibration erroneous data. However, it is worth noting that existing methods mostly rely on the vibration monitoring data of a single bridge. When the target bridge changes, it is still necessary to collect other abnormal samples based on the monitoring data of the target bridge and conduct model training and validation (Zhang *et al*. 2022, Soleimani-Babakamali *et al*. 2022). It is still challenging to directly apply or utilize models trained on a small amount of data between different bridges (Pan *et al*. 2023).

With the residual learning architecture and the introduction of shortcut connectivity, Resnet network solves the problem of gradient vanishing in deep networks. With the advantages of powerful feature extraction and deep learning architecture, it is widely used in many fields such as image classification, target detection, semantic segmentation, face recognition, medical image analysis, remote sensing image processing, generative adversarial networks and video analysis (Wen *et al*. 2020, Tahir *et al*. 2021). To address the above-mentioned issues, a novel bridge vibration data anomaly detection method through ResNet-based feature extraction was proposed with time-efficient classifying and transfer learning. The graphic representations, in type of images, of the monitored time-domain vibration responses are utilized to improve the computation efficiency of anomaly detection. The novelties of the proposed methodology can be summarized as the following two aspects. i) Instead of training a new model from scratch, the pre-trained ResNet50 network is directly utilized to extract the feature vectors from the graphic images of the vibration data. These extracted feature vectors are fed to k-means clustering algorithm to classify the raw examples into different groups. Accordingly, the training dataset can be easily set up with minimum human manipulations. ii) The labelled training dataset are utilized to train the pre-trained ResNet50 network for bridge vibration data anomaly detection. In the sense of transfer learning, the required size of training data can be minimized, at the same time, the detection performance for different bridges can be guaranteed. In this study, the long-term vibration monitoring data recorded by SHM system of Sutong Bridge are utilized to validate the proposed methodology. The obtained conclusions aim to provide technical support for dada-driven condition assessment and maintenance of long-span bridges.

2. Typical examples of the anomalous bridge vibration data

2.1 Description of Sutong Bridge

Sutong Bridge, with a main span of 1,088 meters, was completed and opened to traffic in 2008. The bridge is equipped with a comprehensive SHM system with 399 sensors, e.g., accelerometers, strain gauges, temperature sensors, Global Positioning System (GPS), anemometers, to provide effective data for evaluating the structural operational performance (Wang *et al*. 2016). The vibration monitoring subsystem records the real-time acceleration responses of the main components of the bridge to assess its dynamic performance which is essential for wind-resistance ability evaluation. The accelerometers included in the vibration monitoring subsystem are depicted in Fig. 1. The main girder of the bridge is equipped with 7 pairs (totally 14) bidirectional accelerometers, which comprise acceleration data from 28 channels. The north and south towers are respectively equipped with 1 pair (totally 2) bidirectional accelerometers, which comprise acceleration data from 4 channels. The sampling frequency of the accelerometers are 20 Hz. It should be noted that anomalous data can frequently be found because of the harsh environmental conditions at the bridge site. Therefore, the monitored vibration data of Sutong Bridge can lay the foundation for subsequent data anomaly detection.

2.2 Typical examples of anomalous data

As mentioned in section 2.1, anomalous examples of the monitored bridge vibration data usually occurred due to the

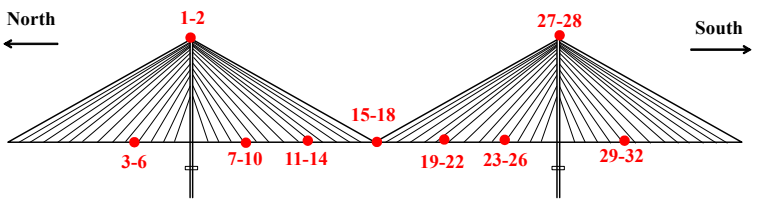

Fig. 1 Layout of the accelerometers included the vibration monitoring subsystem of Sutong Bridge

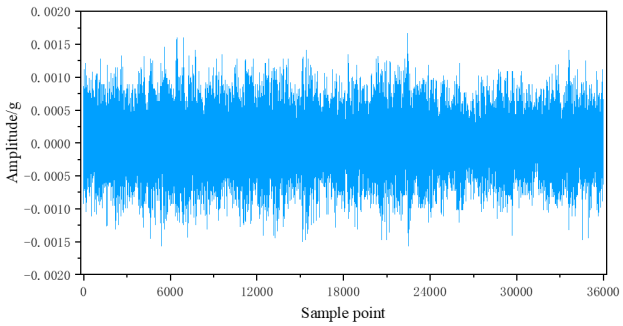

Fig. 2 Normal example of the bridge vibration data

harsh operational environments at the bridge site. The long-term vibration data, totally 32 channels, recorded by the SHM system of Sutong Bridge are reviewed and analyzed. It is well known that the structural acceleration response of the bridge can be considered as a zero-mean Gaussian stationary random process (Ye *et al*. 2023). Therefore, the time history acceleration responses depicted in Fig. 2 should be regarded as reasonable normal examples.

According to the previous studies (Bao *et al*. 2019), the monitored vibration anomalous data can be classified into six categories, i.e., minor, trend, drift, overrange (denoted as square in the following context), outlier, and missing. The typical examples of these corrupted and anomalous data are shown in Fig. 3. Specifically, minor refers to the abnormal amplitude of recorded acceleration response data, which is significantly lower than the normal data amplitude level, and the data type does not exhibit the characteristics of normal acceleration data, often showing a step-like pattern. Trend refers to a significant continuous, steady linear increase or decrease trend in the overall recorded acceleration data. Drift refers to a discontinuous, non-steady linear increase or decrease trend in the recorded acceleration data. Square refers to recorded acceleration data that exceeds the sensor's range of measurement. Outlier refers to the occurrence of single or multiple outliers in the recorded acceleration data. Missing refers to the presence of a substantial amount of missing data or the complete loss of data in the recorded acceleration data. Among the above-mentioned seven categories, outliers exhibit more diverse characteristics, while the remaining six categories have relatively single and distinguishable characteristics. In summary, the vibration monitoring data can be classified into six categories of data anomalies and one category of normal data.

2.3 Graphic transform of the monitored bridge vibration data

For the recorded massive SHM data of the bridges, it is possible to separate anomalous samples based on extracted data features to obtain effective data for structural performance assessment. Previous studies have transformed acceleration time series into images and utilized the deep learning methods with powerful feature analysis capabilities of for data anomaly identification and classification. an overall accuracy ranging from 75% to 94% can be achieved (Chou *et al*. 2022). To improve detection accuracy, researchers have integrated multidimensional feature information from both the frequency domain and time domain, thereby enhancing the accuracy of classifying the anomalous data. However, the generalizability of these methods across different bridge monitoring data can be decreased since the complexity of input images is increased.

This study employs a two-step preprocessing technique for the vibration monitoring data based on deep artificial neural networks to highlight the features that can be

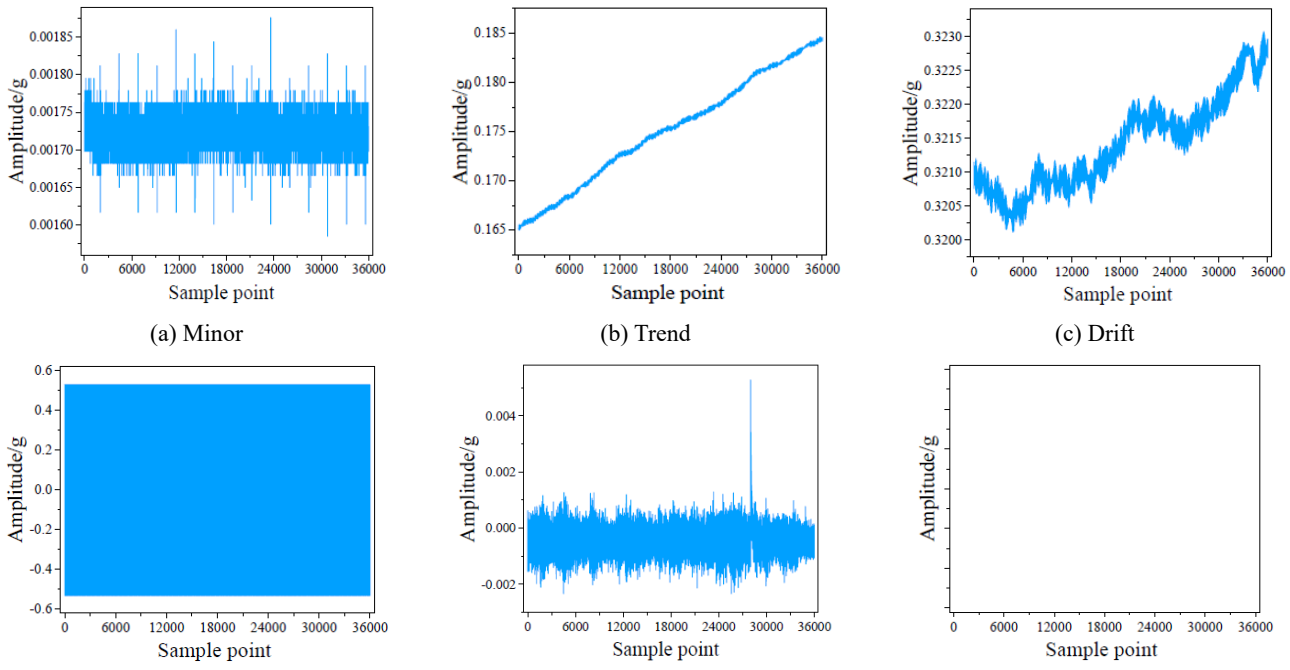

(a) Minor (b) Trend (c) Drift

(d) Square (e) Outlier (f) Missing

Fig. 3 Typical anomalous examples of bridge vibration data

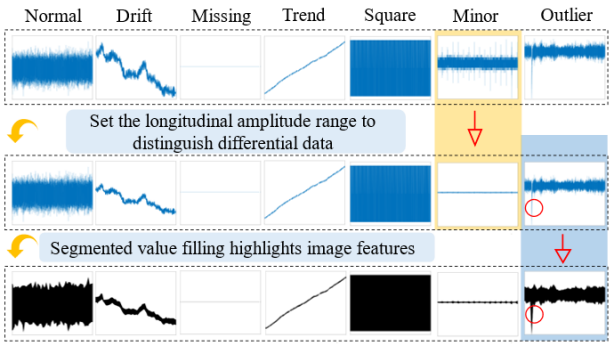

Fig. 4 Two-step preprocessing for transforming the vibration monitoring data into images

extracted for anomaly detection.

(i) In the first step, a minimum amplitude range of the vertical coordinate is set based on the magnitude of the normal acceleration monitoring data. This step is mainly to increase the difference between the normal data image and the minor value data image. Although the minor data image has a lower magnitude than the normal data image, their overall image characteristics are similar with each other. Therefore, an adaptive vertical coordinate range is utilized to generate data images that can mask the differences in magnitude between the two types of data. By comparing the ranging amplitudes between the minor and normal data, one can observe that the absolute value of normal data is 60-80 times that of the minor data. Therefore, when generating data images, a minimum amplitude range of 30 times the range of the minor value is used. After the acceleration data is processed, the original acceleration data is transformed into the images as shown in the second row of Fig. 4. The most obvious change of the minor data highlighted using the yellow background color, consequently, the images of the normal and minor data can be easily distinguished. (ii) In the second step, the sample points are segmented, and the maximum and minimum values within each segment are extracted as control points for the image. Then, the areas within the range of the control points are filled. This step mainly enhances the image features of outliers. When the individual outliers are the plotted as in the image, only two-line segments encompassing a narrow area can be observed, resulting in a low resolution. This feature could mate the outliers difficult to be captured using the computer-vision based methods. Therefore, the original one time-interval data, usually 1 hour, are divided into 60 groups of sub-segments. Then, the maximum and minimum values are extracted from each group of sub-segments, and these values are treated as control points. The area surrounded by the control point data is filled with colors. This process transforms the data image from a stacked line chart into a localized image, highlighting the features of outliers. In Fig. 4, the blue shaded area represents the noticeable features of outlier, indicating that the proportion of pixel points representing outlier values in the image is significantly improved compared to the original image.

In general, using the aforementioned method to process vibration monitoring data makes the image features of minors, outliers, and normal values more distinguishable. This will be beneficial for the subsequent anomaly identification and classification of bridge vibration monitoring data based on computer vision.

3. Framework for time-efficient data labelling and anomaly detection

3.1 Proposed framework

After generating feature-enhanced images, it is necessary to separate the data into different classes according to the rules as shown in Fig. 4 for model training, validation, and testing. Manual labeling is the most widely applied approach, featured as labor-intensive, especially when dealing with large amount of structural health monitoring data. Sometimes, labelling errors usually occurs because of carelessness or exhaustion of the workers. It is observed that each class of bridge vibration data has similar features. This is particularly true for data images with single features related to missing data or data exceeding the range. Therefore, an efficient framework for evaluating the quality of vibration monitoring data is proposed. The framework includes three main parts as shown in Fig. 5.

The first part is an efficient labeling process. Specifically speaking, the first part mainly utilizes the pre-

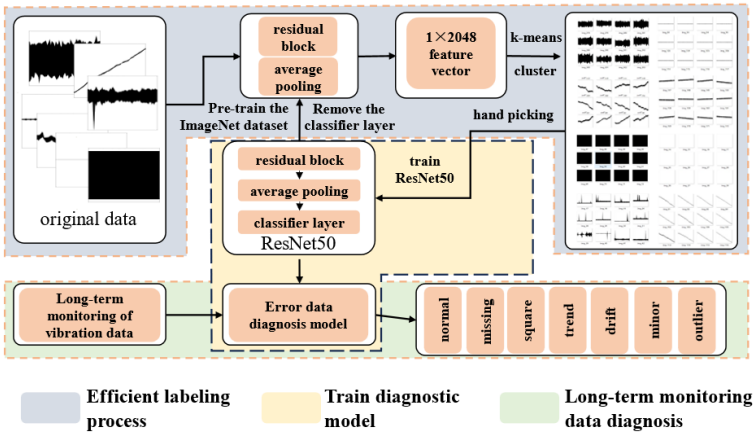

Fig. 5 Proposed framework for efficient anomaly detection of bridge vibration data

trained ResNet50 neural network to extract features from the raw dataset (Tahir *et al*. 2021). The extracted features are then fed into the k-means clustering algorithm to classify the data into different groups. The preliminary classified image sets are then manually adjusted in fine according to Fig. 4 to build the dataset for model training, validation, and testing. In the second part, the labeled dataset is fed into the ResNet50 to train and set up a deep neural network for data anomaly detection. The third part indicates the diagnosis process of the long-term monitored vibration data using the trained model in the second part. The performance of using the initialized model and the pretrained model, namely, transfer learning, to carry out data anomaly detection will be discussed in detail in Section 5.

3.2 Description of ResNet50

Deep convolutional neural networks have been widely applied in image recognition, classification, generation, and other fields. With the increased complexity of image, more complex network structures with large number of convolutional layers are required to extract the high-level image features. It should also be noted that the increased convolutional layers can result in training problems e.g., vanishing gradients and degradation. In other words, the network's classification accuracy becomes difficult to be further improved when the convolutional layers reach a certain depth. To address this issue, He *et al*. (2016) introduced the concept of residual networks, denoted as ResNet, in which the weight layers learn residual functions with reference to the layer inputs.

In a conventional stacked artificial neural network, one layer can be represented as learning a function $y = F(x)$, where x is the input of that layer, y is the output of that layer (i.e., observed value), and $F(x)$ represents the learned relationship between the input and output values. In contrast, a residual network adopts skip connections, which directly transmit the input x to the output position and establish a connection with the output. This transforms the learning process of the model from $y = F(x)$ to $f(x) = F(x) – x$, where $f(x)$ represents the residual.

The utilization of residual networks addressed the challenges in network optimization, gradient vanishing, and degradation, resulting in a significant improvement in image classification accuracy. After conducting a thorough comparison of types and the depth of residual networks, this research selects ResNet50 as the foundational model for bridge vibration data anomaly detection.

Fig. 6 illustrates two types of residual blocks in the ResNet50 neural network, showcasing the direct connections that exist between the input and output. This characteristic defines the essence of residual networks. As shown in Fig. 7, ResNet50 consists of two types of residual blocks, totaling 16 blocks in the entire network structure, spanning a total of 50 layers. The default size of the input image to the ResNet50 model is a 224 × 224 × 3 pixel. After passing through the residual blocks with convolutional layers, average pooling is performed, followed by a connection to the fully connected layer for classification.

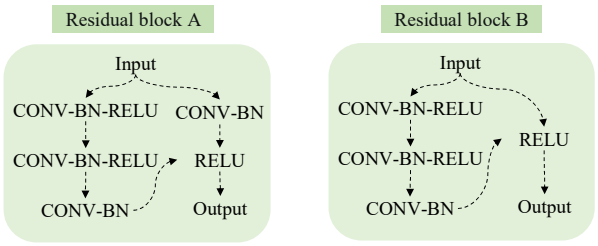

(a) Block A (b) Block B

Fig. 6 Illustration of the residual blocks in ResNet50

3.3 Feature extraction of the generated images

Generally, the pixel array of the visualized image of vibration monitoring data can directly be used for the subsequent cluster analysis but may pose additional challenges. The redundant information imbedded in the pixel array of the data image will not contribute to the accuracy of clustering but will greatly decrease the computation efficiency. The ResNet50 is utilized to extract meaningful features from the raw generated image. As outlined in Section 2.4, ResNet50 produces a feature map with dimensions 7 × 7 × 2048 following its passage through the convolution layers within the residual blocks. Following this, average pooling is employed to derive a feature vector sized 1 × 2048, which is subsequently input into the classifier for classification.

The original ResNet50, pretrained on the ImageNet dataset, is designed to extract the high-level features for discriminating among 1000 classes of images. Likewise, in this study, we utilize the pretrained ResNet50 neural network weights for extracting features from vibration monitoring data images, resulting in a feature vector of dimensions 1 × 2048. Following this, clustering analysis is

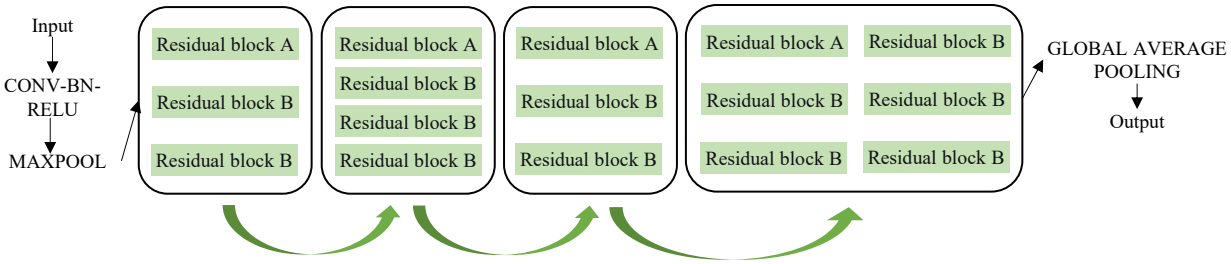

Fig. 7 Illustration of the overall structure of ResNet50

employed on the feature vector of vibration monitoring data images to attain more precise clustering outcomes, thereby facilitating the preliminary classification of the intricate dataset.

3.4 Preliminary classification of the bridge vibration data with k-means clustering

The *k*-means clustering is an unsupervised machine-learning method that minimizes the relationships between data to reduce the loss function, achieving the partition of sample data into *k* clusters (Hartigan and Wong 1979). Its loss function is defined as the sum of squared distance errors between each sample point and the centroid of its assigned cluster. This method assigns samples to the cluster with the nearest distance, indicating the category of the sample as the cluster with the closest distance.

The determination of *k* in the *k*-means clustering algorithm is particularly important. The elbow method is usually used to assist in the determination process. It involves calculating the average within-cluster sum of squares for different values of *k* and plotting them on a line chart. The optimal value of *k* can then be determined by identifying the "elbow" or the point of inflection on the chart. In the case of bridge vibration monitoring data, previous studies (Bao *et al*. 2018, 2019) reported seven data classes, which will be also considered as one factor except for elbow chat, when determining the appropriate *k* value.

In this study, the pretrained ResNet50 is initially utilized to extract feature vectors from the bridge vibration monitoring data. Subsequently, the k-means algorithm is employed to classify these feature vectors. The relationship between average deviation and the number of clustering clusters *k* during cluster analysis is depicted in Fig. 8. Notably, a discernible inflection point is observed at $k = 8$, aligning closely with the seven categories of bridge vibration monitoring data identified through manual analysis in Section 2.2. Consequently, we opt for the value $k = 8$ for the preliminary classification of the dataset.

The classified results with $k = 8$, shown in of Fig. 5, demonstrate that the *k*-means clustering algorithm can successfully grouped similar feature data together. Based on the obtained eight clusters, the bridge vibration monitoring data can be easily and efficiently classified into the eight data types, i.e., outliers, normal, minor, minor with slight trend, drift, square, trend, and missing. It is worth noting that minor and minor with slight trend are both considered as minor in previous studies (Bao *et al*. 2018). Therefore, in this study, this unsupervised learning method, i.e., *k*-means clustering, also classifies the bridge vibration data into seven classes as shown in Fig. 4.

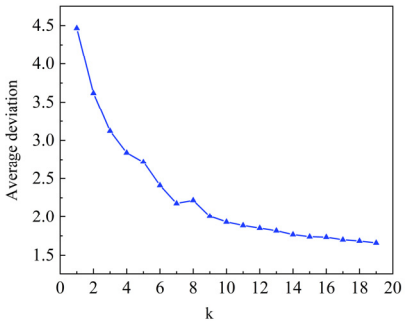

Fig. 8 Variation of average deviation with the increased cluster number

After conducting a statistical analysis, the distribution of primary data types in various categories is presented in Table 1. It is evident that the accuracy for outliers, square, trend, and missing data surpasses 99% in each respective category, indicating commendable performance. However, the clustering results for drift data exhibit a less favorable accuracy, reaching only 74.4%. Notably, the clustering results are not completely satisfactory. And the accuracy of the clustering results only represents the ratio of the number of each specific data image type in each cluster to the number of all images in that cluster, and does not know the true number of each type of data. The k-means clustering algorithm is not suitable to be directly used for data anomaly detection. Based on the clustering results, preliminary classified data can be obtained as input for supervised learning, which effectively mitigating the laborious task of manual labeling. Accordingly, the dataset is divided into training set, validation set and test set to develop accurate data anomaly detection neural network.

4. Quality evaluation of the monitored vibration data of Sutong Bridge

The annotated bridge vibration monitoring data is used to train the ResNet50 model for setting up an efficient data anomaly detection framework. Two distinct models, namely Model A and Model B, are separately trained. Model A is trained by utilizing vibration monitoring data images with a restricted amplitude range. Subsequently, diagnostic Model B is trained by employing vibration monitoring data images with both a restricted amplitude range and enhanced pixels through segmented padding for highlighting features in the images. One should observe that the inputs for both models are derived from the same raw vibration monitoring data but undergo distinct preprocessing procedures. Subsequently, comprehensive comparison of metrics is conducted between Model A and Model B. Finally, the obtained two models are used to evaluate the quality of long-term vibration monitoring data of Sutong Bridge.

4.1 The adopted evaluation criteria

The evaluation metrics for the image classification

Table 1 The ratio of classified data types of bridge vibration responses

Data types	Outlier	Normal	Minor	Minor with slight trend	Square	Trend	Missing	Drift
Ratio (%)	99.8	91.0	94.1	83.2	99.8	99.8	99.8	74.4

model primarily include precision, recall, and F1 score, which will be briefly introduced in the following sections (Hossin and Sulaiman 2015).

(1) Precision

Precision represents the proportion of samples predicted as positive instances that are actually positive and can be expressed as Eq. (1)

$$Precision = \frac{TP}{TP + FP} \tag{1}$$

where *TP* represents the positive examples predicted as the positive, and *FP* represents the quantity of negative samples predicted as the positive.

(2) Recall

Recall refers to the proportion of one class samples predicted as the true label and can be calculated using Eq. (2).

$$Recall = \frac{TP}{TP + FN} \tag{2}$$

where *FN* represents the quantity of positive samples predicted as the negative.

(3) F1-Score

As usual, higher precision and recall values indicate a better classification performance of the obtained model. It is difficult to achieve the highest points for both precision and recall. Therefore, the F1-Score serves as a metric to balance recall and precision values to obtain the optimal model and can be calculated using Eq. (3).

$$F1 - Score = \frac{2 \times Recall \times Precision}{Recall + Precision} \tag{3}$$

The above-mentioned three metrics, i.e., precision, recall, and F1-Score, are useful criteria for evaluating classification performance of the trained neural network models. The selected optimal model can serve as effective tool to detect the anomalous example of the bridge vibration data.

4.2 Network training

Based on the above analysis, the quantity of outliers is relatively low among the seven identified data categories. Therefore, within the dataset, each of the six categories—normal, minor, trend, drift, square, and missing data—comprises 1000 image samples, while the outlier category includes 500 image samples. These samples are proportionally divided into training and validation sets at a ratio of 4:1, as depicted in Table 2. The neural network is trained with a batch size of 16, over 200 epochs. The dimension of the input image is 112 × 112 × 3.

The variation of accuracy when training Model A and Model B is plotted Fig. 9. When the epoch reaches 100, Model A achieves its highest accuracy, maintaining stability with the validation set's peak accuracy at 94.5%. Similarly, when the epoch reaches 70, Model B attains its highest accuracy, remaining stable with the validation set's peak accuracy at 96.9%. Overall, the structures of the two models are identical; however, during training, Model B exhibited faster convergence speed and achieved a higher predictive accuracy compared with Model A. This can be attributed to the image enhancement in Model B, where training data underwent amplitude restriction and segmented padding to augment pixels, demonstrating the effectiveness of feature enhancement in vibration monitoring data images.

Furthermore, utilizing the acceleration data recorded by the SHM system of the Sutong Bridge, 37,427 sample sets were generated to assess the capabilities of Model A and Model B on bridge vibration data anomaly detection. The confusion matrices of the two models' prediction outcomes are depicted in Fig. 10, which indicates overall favorable predictive accuracy. Remarkably, the predictions for the

Table 2 The number of samples for training and validation

Sample number \ Data types	Normal	Trend	Minor	Drift	Square	Outlier	Missing
For training	800	800	800	800	800	400	800
For validation	200	200	200	200	200	100	200
Total	1000	1000	1000	1000	1000	500	1000

(a) Model A (b) Model B

Fig. 9 Variation of the accuracy during the training process

categories of missing and square exhibited highest accuracy. In the confusion matrix of Model A, the maximum number of images causing confusion in predictions between minor and normal data was 19. In contrast, in the confusion matrix of Model B, this confusion was reduced to a maximum of only 8 images, demonstrating that the segmented padding in vibration monitoring data successfully enhanced the image features of each class of bridge vibration data. Subsequently, precision, recall, and F1 scores were computed for each data category to comprehensively evaluate the models' predictive performance.

The precision of Model A and Model B, analyzed using the test set, is listed in Table 3. Both models demonstrate commendable diagnostic precision, with Model B exhibiting a slightly higher overall predictive precision of 98.14% compared with Model A, i.e., 97.12%. For each data category, Model A shows relatively high precision in predicting missing, normal, trend, drift, minor, and square data, all exceeding 93%. However, its precision in predicting outlier values is lower at 68.82%. This aligns with findings by Bao *et al*. (2018), where they observed that the image features of outlier values bear resemblance to normal and minor data, leading to potential misdiagnosis in deep learning models. The observation is consistent with results depicted in Fig. 10(a).

It is evident that Model B exhibits relatively high precision in predicting missing, normal, trend, drift, minor, and square data, all exceeding 96%. This represents a noticeable improvement compared with Model A, with a significant reduction in the misidentification rate, particularly for outlier values. Model B achieves a precision rate of 85.56% for predicting outlier values, marking a notable improvement of 16.74% compared with Model A.

The recall rates for predicting the test set by Model A and B are listed in Table 4. The recall rates for Model A generally align with the precision rates. Specifically, the recall rates for six types of data, i.e., missing, normal, trend, drift, minor, and square, are all above 95.82%, with the recall rate for outlier values at 79.19%. Model B surpasses Model A in recall rates, notably achieving an 84.99% recall rate for outlier values, reflecting a noteworthy improvement of 5.8%.

F1 scores, which comprehensively consider both precision and recall, for Model A and B are summarized in Table 5. Similar to previous findings, the F1 scores for Model B are slightly higher than those of Model A. Remarkably, Model B attains an F1 score of 84.99% for outlier values, showcasing an improvement of 11.35% over the Model A of 73.64%.

Overall, the preprocessing of the original vibration data has comprehensively enhanced the performance of the established ResNet network. In particular, the reliability of

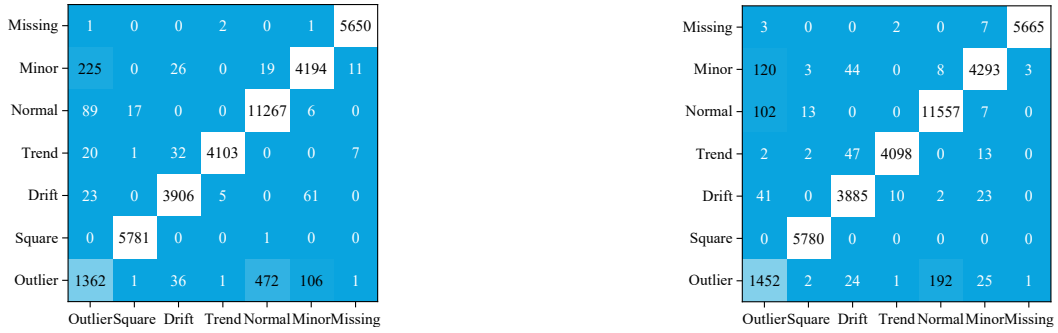

(a) Model A (b) Model B

Fig. 10 Confusion matrices of the predicted results by Model A and B

Table 3 The precision of the predicted results of testing dataset

Data types / Sample number	Missing	Minor	Normal	Trend	Drift	Square	Outlier	All
Model A	0.9993	0.9372	0.9902	0.9856	0.9777	0.9998	0.6882	0.9712
Model B	0.9979	0.9602	0.9896	0.9846	0.9808	1.0000	0.8556	0.9814
ΔAB	-0.0014	0.0230	-0.0006	-0.0010	0.0031	0.0002	0.1674	0.0102

* Note: ΔAB is the indicator difference of Model A and Model B

Table 4 The recall rate of the predicted results of testing dataset

Data types / Sample number	Missing	Minor	Normal	Trend	Drift	Square	Outlier	All
Model A	0.9966	0.9602	0.9582	0.9981	0.9765	0.9967	0.7919	0.9689
Model B	0.9986	0.9714	0.9862	0.9907	0.9760	0.9983	0.8499	0.9814
ΔAB	0.0020	0.0112	0.0280	-0.0074	-0.0005	0.0015	0.00580	0.0125

Table 5 The F1 scores of the predicted results of testing dataset

F1 scores \ Data type	Missing	Minor	Normal	Trend	Drift	Square	Outlier	All
Model A	0.9980	0.9485	0.9739	0.9918	0.9771	0.9983	0.7364	0.9698
Model B	0.9986	0.9714	0.9862	0.9907	0.9760	0.9983	0.8499	0.9813
ΔAB	0.0006	0.0229	0.0123	-0.0011	-0.0011	0.0000	0.1135	0.0115

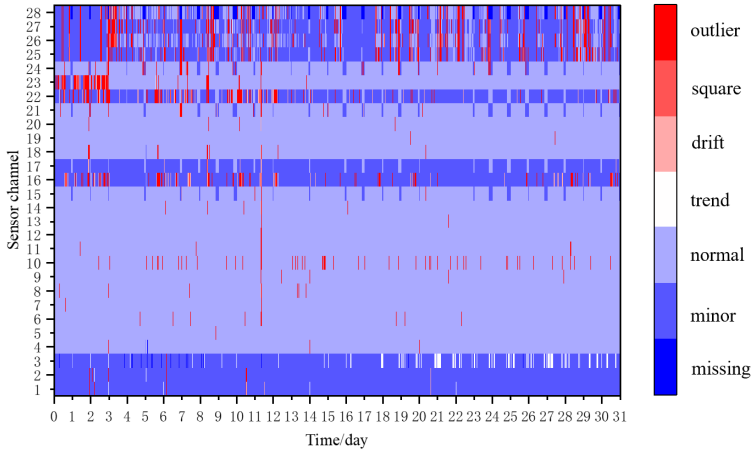

Fig. 11 The quality of the monitored vibration data of the main girder of Sutong Bridge

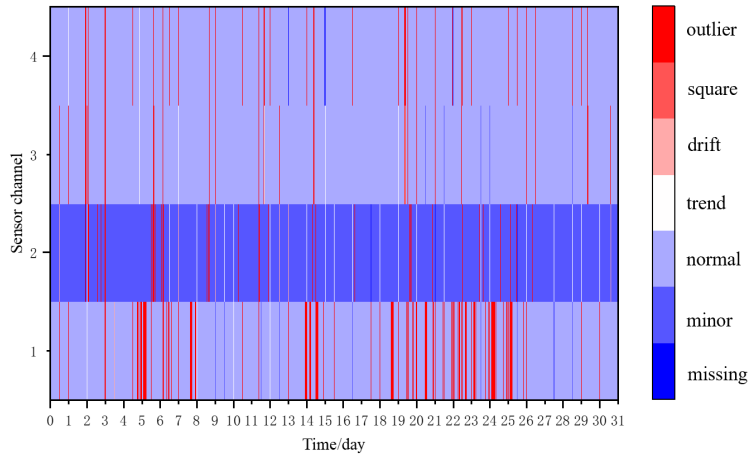

Fig. 12 The quality of the monitored vibration data of the main tower of Sutong Bridge

detection of outliers in bridge vibration monitoring data has been significantly improved. Therefore, the obtained Model B will be utilized to carry out the subsequent analysis.

4.3 Quality evaluation of monitored one-month bridge vibration data

The SHM system of Sutong Bridge incorporates 16 acceleration sensors, constituting a total of 32 channels. These acceleration sensors continuously record a substantial amount of vibration data to sense the vibrational performance of the main girder and towers under the influence of wind and vehicle loads. In this section, Model B will be utilized to assess the quality of the acceleration data recorded by the SHM system of Sutong Bridge over a one-month period (July 2012). The objective is to lay the foundation for subsequent tasks, including modal parameter identification, operational performance assessment.

Fig. 11 depicts the results of the data quality assessment for the 28 channels of acceleration sensors installed on the main girder of Sutong Bridge. During the monitoring period, it can be observed that the data from the majority of channels (Channels 4-15, 18-21, and Channel 23) exhibit a normal state, intermittently interspersed with outliers. Anomalous data tends to concentrate, with the first three channels predominantly comprising minor and trend datatypes. Channels 16-17 primarily exhibit minor and outlier datatypes. Channels 22 and 25-28 predominantly contain minor, outlier, and missing datatypes. Overall, the proportion of anomalous data is relatively high after four

years of service, significantly impairing the effective functioning of the bridge's SHM system.

The quality assessment results for the acceleration monitoring data of the main tower of the bridge are depicted in Fig. 12. One can observe that the acceleration monitoring data of the main towers is mostly composed of normal values, interspersed with intermittent occurrences of outlier value and trend data. The data type for Channel 2 of the bridge tower is primarily minor, with a slight mixture of outlier and trend data.

Based on the quality assessment results of the acceleration monitoring data for the main girder and towers of Sutong Bridge, the following preliminary conclusions can be drawn. (i) Due to harsh service conditions, the anomalous proportion of the monitored bridge acceleration data is relatively high, and once anomalies occur, the data often struggle to automatically recover operational performance. (ii) Minor and outlier values are the most common anomalous types of bridge vibration data. (iii) The monitored bridge acceleration data intermittently generate outlier values, intermingling with normal data, thus affecting the assessment of the subsequent bridge's operational performance evaluation based on vibration monitoring data.

5. Discussion on transfer learning for data anomaly detection

5.1 Concept of transfer learning for ResNet50

The study utilizes a deep artificial neural network, specifically ResNet50, to perform anomaly diagnosis on bridge vibration data. In general, a well-structured and adequately large dataset plays a crucial role in enabling the trained model to capture intricate feature patterns within the samples. This capability allows the model to accurately identify and classify abnormal patterns present in bridge vibration data. In the initial analysis, it was noted that the abnormal patterns in vibration monitoring data differ across various locations of the bridge. Specifically, there is a higher abundance of effective samples for normal and outlier values, whereas there is a scarcity of samples for unusual data patterns such as square, missing, trend, and drift. This observation is particularly prominent in the monitoring data generated by the new implemented SHM system for the bridge. The proposed concept of transfer learning (Weiss *et al*. 2016, Zhuang *et al*. 2020, Zhang and Yuen 2021) provides an effective alternative to addressing these challenges. Transfer learning aims to leverage datasets from similar or identical tasks to pre-train deep artificial neural networks. Subsequently, the pre-trained network is applied to a new task, requiring only a small dataset specific to that task for fine-tuning. This process enables achieving improved classification and prediction accuracy. Therefore, this section will utilize the pre-trained deep neural network, namely ResNet50 (Wen *et al*. 2020), to conduct anomaly diagnosis for bridge vibration data and discuss the applicability of transfer learning.

The transfer learning approach for ResNet50 is illustrated in Fig. 13, comprising the following two main steps. ① ResNet50 is trained using the publicly available ImageNet dataset to achieve a high accuracy for image classification. At this point, the left shaded portion of the network layers in Fig. 13 has acquired proficient image feature extraction capabilities. Consequently, the weights of this portion of the network are frozen for subsequent transfer learning. ② The feature extraction layer, with its weights fixed, is integrated with the classification layer network (the right shaded portion in Fig. 13). Subsequently, a limited set of bridge vibration monitoring data is employed as training samples to fine-tune the relevant weight coefficients. This process enables the anomaly diagnosis and classification of bridge vibration monitoring data.

5.2 Discussion on the performance of transfer learning

This section will comprehensively analyze the impact of the training set size on the anomaly detection accuracy based on transfer learning. Effective sample sizes for each data category are set to 20, 50, 70, 100, 150, 200, 300, and 400 images, with a consistent training-to-validation set ratio of 4:1 for each group of data. The pre-trained ResNet50 is then fine retrained until convergence for anomaly detection of bridge vibration monitoring data. Utilizing the obtained transfer learning models for prediction, testing is conducted on a consistent test set, as mentioned in Section 2.5, similar to Model B, and confusion matrices are obtained. Furthermore, precision, recall, and F1 scores for different transfer learning models are computed, and the results are illustrated in Figs. 14, 15 and 16.

Fig. 14 illustrates the relationship between the precision of the transfer learning network and the size of training dataset for each class. The red dashed line in the graph represents the precision of original model from Section 4.2. As observed from the graph, the precision of the transfer

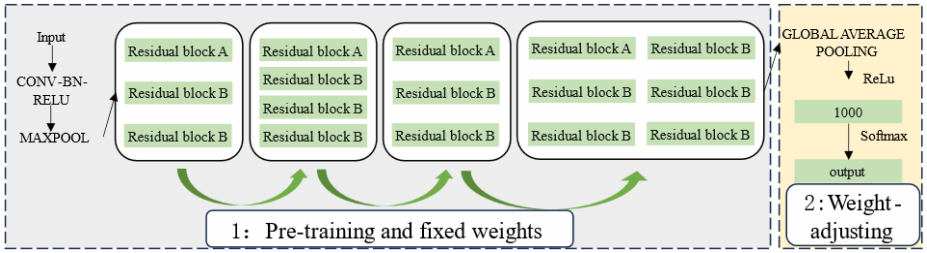

Fig. 13 The framework of transfer learning for ResNet50

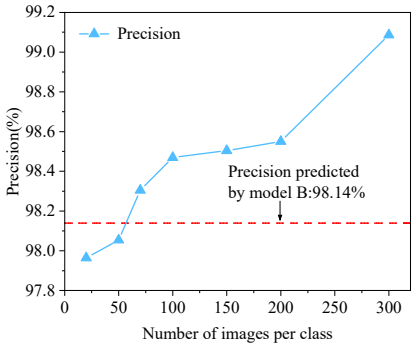

Fig. 14 The precision of the predicted results of testing dataset using transfer learning

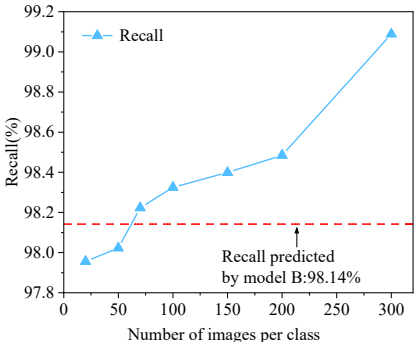

Fig. 15 The recall rate of the predicted results of testing dataset using transfer learning

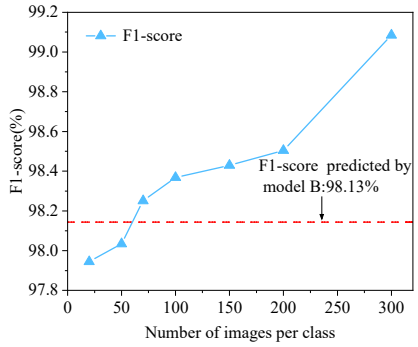

Fig. 16 The F1 scores of the predicted results of testing dataset using transfer learning

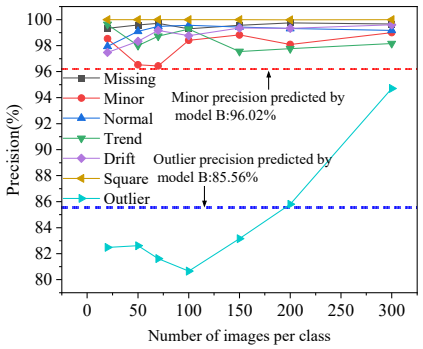

Fig. 17 The precision of the obtained transfer learning model for each data class

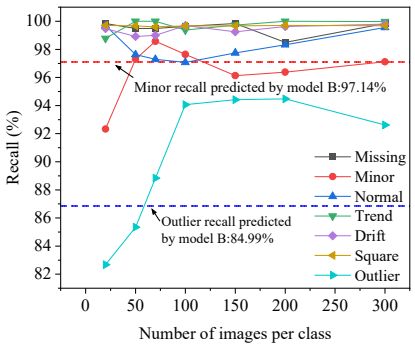

Fig. 18 The recall rate of the obtained transfer learning model for each data class

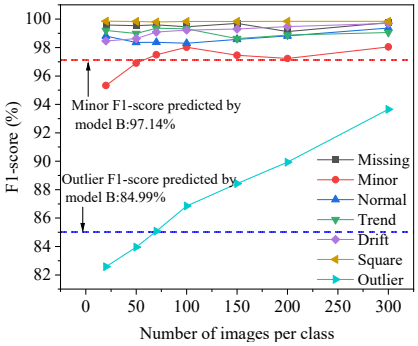

Fig. 19 The F1-score of the obtained transfer learning model for each data class

learning model improves with an increase in the size of training dataset. When the number of samples for each class reaches 70 (a total of 490 samples for 7 classes), the predictive accuracy of the transfer learning model reaches 98.3%, surpassing the precision of Model B, i.e., 98.14%.

Fig. 15 depicts the relationship between the recall of the transfer learning network and the size of training dataset for each class. The red dashed line in the graph represents the recall of Model B from Section 4.2. As evident from the graph, the change in recall for the transfer learning network follows a pattern like precision. The recall gradually increases with the growth in the size of training dataset. When the number of samples for each class reaches 70 (a total of 490 samples for 7 classes), the predictive recall of the transfer learning model reaches 98.23%, surpassing the recall of Model B, i.e., 98.14%.

Fig. 16 illustrates the relationship between the F1-score of the transfer learning model and the size of training dataset for each class. As observed from the graph, the pattern of change in the F1-score for the transfer learning network is like the two previous indicators. The F1-score gradually increases with the growth in the number of training set samples. When the number of samples for each class reaches 70 (a total of 490 samples for 7 classes), the F1-score of the transfer learning model has reached 98.27%, surpassing the F1-score of Model B, which is 98.13%.

It is noteworthy that Model B has a training sample size of 6500, which is 13.26 times the size of the transfer learning model. The transfer learning model achieved

higher precision, recall, and F1-score with significantly fewer training samples compared with Model B.

Next, we will further analyze the reliability of the transfer learning model in identifying various anomalies in bridge vibration monitoring data. Precision, recall, and F1 scores for each data class were calculated based on the test set of Model B. The indicators for the "minor value" and "outlier" data categories, which showed significant changes, were compared with the results of Model B. The results are illustrated in Figs. 17 to 19.

Fig. 17 illustrates the variation of the precision of the transfer learning model for predicting the seven categories of bridge vibration monitoring data with changed size of training dataset. It is observed that the precision of the "missing," "trend," "square," "drift," and "normal" data categories does not show significant changes with the increase in training sample size. The precision of the "minor value" category experiences minor fluctuations before stabilizing.

In general, these six types of data exhibit relatively simple features, making them easy for the transfer learning model to learn. Notably, when the training sample data is limited, the precision of the "outlier" category is only slightly higher than 80%. Yet, with the increase in the training sample size, especially when the single-category training sample size reaches 200 (a total of 1400 samples for seven categories), the precision consistently surpasses that of Model B (85.56%) and continues to improve with the growth of training samples.

Similarly, as observed in Figs. 18 and 19, the recall and F1 scores of the transfer learning model follow similar patterns. Slightly different, however, is that the recall and F1 scores for the "minor value" category gradually increase to a stable level only when the single-category training sample size exceeds 50.

The above results indicate that the transfer learning model achieves good accuracy in diagnosing anomalous data with relatively few training samples. However, the diagnostic accuracy for outlier values and minor values may still be weaker than that of Model B. As the training sample size of transfer learning model increases to a certain level (i.e., single-category sample size of 200, total of 1400 samples for 7 categories), the prediction accuracy for outlier values and minor values can effectively surpass that of Model B.

This is attributed to the exceptionally complex image features of outlier value data in acceleration monitoring. The organic combination of a pre-trained transfer learning model and few training samples contributes to enhancing the predictive performance of artificial neural networks. In summary, the transfer learning model, utilizing a training sample size significantly smaller than that of Model B, demonstrates a reliable capability for anomaly diagnosis in bridge vibration monitoring data.

5.3 Comparison of models and generalized performance verification

To verify the superiority and the detection performance of the model in this study, 5 different models, including

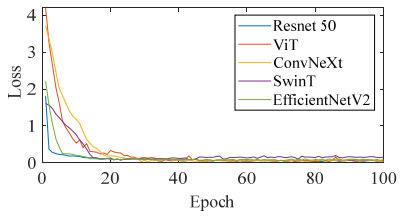

(a) The training process of different models

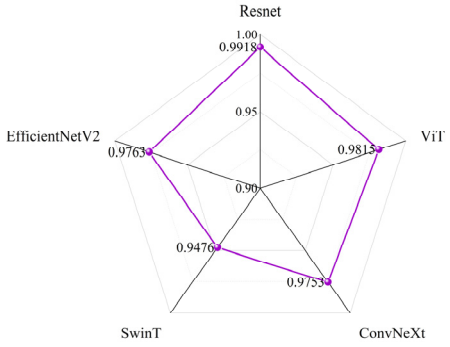

(b) Accuracy comparison of of different models

Fig. 20 The detection performance comparison of the different models

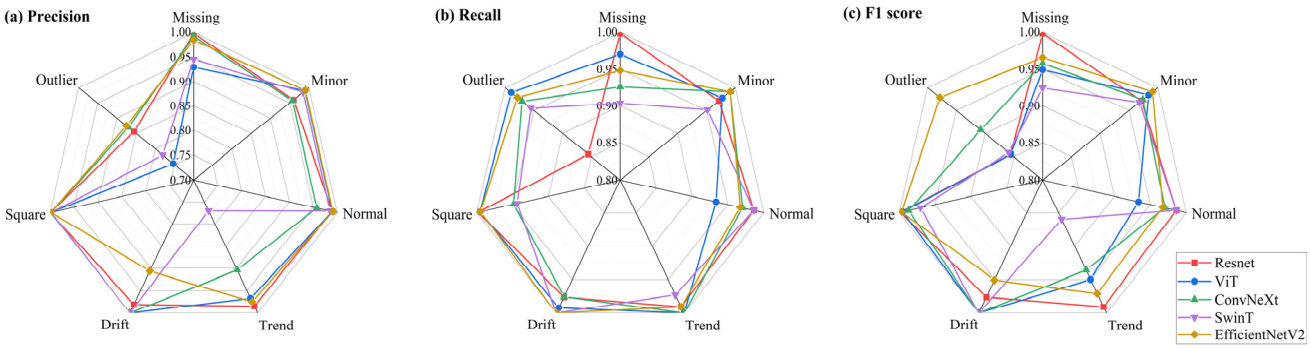

Fig. 21 Evaluation indicators of each model

(a) Loss curve of the training process

(b) Accuracy curve of the training process

Fig. 22 Transfer learning model training process curve

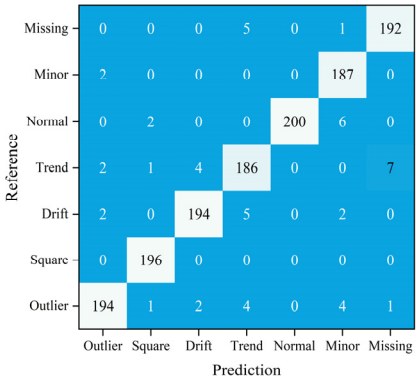

Fig. 23 The confusion matrix obtained from the test data

Vision Transformer (ViT) (Wang *et al*. 2021), Pure Convolutional Neural Network (ConvNeXt) (Shi *et al*. 2024), Swin Transformer (SwinT) (Liu *et al*. 2021), EfficientNetV2 (Long *et al*. 2023) and the Model B proposed in this paper is compared. As shown in Fig. 20, the model proposed in this paper converges faster and is more computationally efficient compared to other models due to the simultaneous extraction of features from both data and images and the use of migration learning methods. Evaluation indicators of the models are shown in Fig. 21. In contrast, the anomaly detection ability of the model in this study is relatively better than other models in terms of trend, missing and square. Its three metrics for anomaly detection of missing reached 99.86%, 99.79%, 99.86%. The EfficientNetV2 model achieves 99.1%, 96.6%, and 99.1% for minor anomaly detection, respectively, which is the best performance. The model proposed in this paper can be further improved in detecting anomaly data such as outlier. The lightness of the model is much less than other models. As a result, the model requires less configuration of the operating equipment and has a wider range of applications.

In addition, the ResNet transfer learning model used for bridge vibration data anomaly detection in this study is transferred to the Nanjing Qixia Mountain Yangtze River Bridge (NQYRB) to verify the generalizability. The NQYRB has three spans with lengths of 576.2 m, 1418 m and 481.8 m and ranked third among similar bridges in the world at that time. During the long-term vibration monitoring of the main girder and suspenders, large amount of abnormal data in their monitoring data were observed (Mao *et al*. 2023). For this reason, the method proposed in this study is used to detect abnormal data. Specifically, 500 groups of abnormal data are selected for each category, and a total of 3500 groups of abnormal data are used for model training, and their training curves are shown in Fig. 22. The confusion matrix obtained from the test data are shown in Fig. 23.

It can be observed that when the number of training rounds of the model reaches 80, the accuracy of the training and validation sets no longer increases and the model accuracy reaches 97.5%. The results are close to those obtained on the Sutong Bridge, indicating that the transfer learning approach can effectively transfer the knowledge of the model to a new dataset. The confusion matrix shows the positive performance of the model on the NQYRB, which verifies the applicability of the model in the new environment.

6. Conclusions

- The proposed efficient feature-based labeling process, utilizing the pre-trained ResNet50 and k-means clustering, can help to classify the raw dataset into different groups. Based on these outcomes, preliminary classification with relatively high accuracy can be obtained; hence effectively mitigating the laborious task of manual labeling for training the deep neural network to detect the anomalous bridge vibration data.
- Before transforming the timeseries bridge vibration data into graphs, the two-step preprocessing of the original vibration data, involving amplitude limitation and segment-wise padding for enhanced pixel density, has comprehensively enhanced the performance of the established ResNet network. Particularly noteworthy is the significant improvement in the detection reliability of outlier values within the bridge vibration monitoring data.
- The combination of a pre-trained transfer learning model and few valid training samples contributes to enhancing the predictive performance of the established deep learning networks. In other words, the transfer learning model, utilizing a training sample size significantly smaller than that of Model B, demonstrates a reliable capability for anomaly diagnosis in bridge vibration monitoring data. The model shows positive performance in comparison with state-of-the-art models as well as in generalization validation.

Acknowledgments

The authors would like to gratefully acknowledge the support from National Key R&D Program of China (2022YFB3706704), National Natural Science Foundation of China (52378291, 524B2126, 52108274), and Academician Project Foundation of CCCC (YSZX-01-2022-01-B).

References

Annamdas, V.G.M., Bhalla, S. and Soh, C.K. (2017), "Applications of structural health monitoring technology in Asia", *Struct. Health Monitor.*, **16**(3), 324-346. https://doi.org/10.1177/1475921716653278

Bao, Y., Tang, Z., Li, H. and Zhang, Y. (2018), "Computer vision and deep learning–based data anomaly detection method for structural health monitoring", *Struct. Health Monitor.*, **18**(2), 401-421. https://doi.org/10.1177/1475921718757405

Bao, Y., Chen, Z., Wei, S., Xu, Y., Tang, Z. and Li, H. (2019), "The state of the art of data science and engineering in structural health monitoring", *Engineering*, **5**(2), 234-242. https://doi.org/10.1016/j.eng.2018.11.027

Catbas, F.N., Susoy, M., and Frangopol, D.M. (2008), "Structural health monitoring and reliability estimation: Long span truss bridge application with environmental monitoring data", *Eng. Struct.*, **30**(9), 2347-2359. https://doi.org/10.1016/j.engstruct.2008.01.013

Chou, J.Y., Fu, Y., Huang, S.K. and Chang, C.M. (2022), "SHM data anomaly classification using machine learning strategies: A comparative study", *Smart Struct. Syst., Int. J.*, **29**(1), 77-91. https://doi.org/10.12989/sss.2022.29.1.077

Du, Y., Li, L.F., Hou, R.R., Wang, X.Y., Tian, W. and Xia, Y. (2022), "Convolutional neural network-based data anomaly detection considering class imbalance with limited data", *Smart Struct. Syst., Int. J.*, **29**(1), 63-75. https://doi.org/10.12989/sss.2022.29.1.063

Entezami, A., Sarmadi, H. and Behkamal, B. (2023), "Long-term health monitoring of concrete and steel bridges under large and missing data by unsupervised meta learning", *Eng. Struct.*, **279**, 115616. https://doi.org/10.1016/j.engstruct.2023.115616

Figueiredo, E. and Brownjohn, J. (2022), "Three decades of statistical pattern recognition paradigm for SHM of bridges", *Struct. Health Monitor.*, **21**(6), 3018-3054. https://doi.org/10.1177/14759217221075241

Fu, Y., Peng, C., Gomez, F., Narazaki, Y. and Spencer Jr, B.F. (2019), "Sensor fault management techniques for wireless smart sensor networks in structural health monitoring", *Struct. Control Health Monitor.*, **26**(7), e2362. https://doi.org/10.1002/stc.2362

Hartigan, J.A. and Wong, M.A. (1979), "Algorithm AS 136: A k-means clustering algorithm", *J. Royal Statist. Soc. Series C (Appl. Statist.)*, **28**(1), 100-108. https://doi.org/10.2307/2346830

He, K., Zhang, X., Ren, S. and Sun, J. (2016), "Deep residual learning for image recognition", In: *Proceedings of the IEEE Conference on Computer Vision and Pattern Recognition*, Las Vegas, NV, USA, pp. 770-778.

Hossin, M. and Sulaiman, M.N. (2015), "A review on evaluation metrics for data classification evaluations", *Int. J. Data Min. Knowl. Manag. Process*, **5**(2), 1.

Liu, Z., Lin, Y., Cao, Y., Hu, H., Wei, Y., Zhang, Z., Lin, S. and Guo, B. (2021), "Swin transformer: Hierarchical vision transformer using shifted windows", In: *Proceedings of the IEEE/CVF International Conference on Computer Vision*, pp. 10012-10022.

Long, J.N., Zhang, Z., Liu, X.H., Li, Y.X., Rui, Z.Y., Yu, J.F., Zhang, M., Flores, P., Han, Z.X., Hu, C. and Wang, X.F. (2023), "Wheat Lodging Types Detection Based on UAV Image Using Improved EfficientNetV2", *Smart Agricul.*, **5**(3), 62-74. https://doi.org/10.12133/j.smartag.SA202308010

Mao, J.X., Wang, H. and Spencer Jr, B.F. (2021), "Toward data anomaly detection for automated structural health monitoring: Exploiting generative adversarial nets and autoencoders", *Struct. Health Monitor.*, **20**(4), 1609-1626. https://doi.org/10.1177/1475921720924601

Mao, J.X., Su, X., Wang, H. and Li, J.Y. (2023), "Automated Bayesian operational modal analysis of the long-span bridge using machine-learning algorithms", *Eng. Struct.*, **289**, 116336. https://doi.org/10.1016/j.engstruct.2023.116336

Memisoglu, N.A., Zulfikar, A.C. and Cetindemir, O. (2022), "Structural health monitoring systems of long-span bridges in Turkey and lessons learned from experienced extreme events", *J. Civil Struct. Health Monitor.*, **12**(6), 1375-1412. https://doi.org/10.1007/s13349-022-00551-x

Mondal, T.G., Chou, J.Y., Fu, Y. and Mao, J. (2023), "A hybrid deep neural network compression approach enabling edge intelligence for data anomaly detection in smart structural health monitoring systems", *Smart Struct. Syst., Int. J.*, **32**(3), 179-193. http://dx.doi.org/10.12989/sss.2023.32.3.179

Ni, Y.Q., Wang, Y.W. and Zhang, C. (2020), "A Bayesian approach for condition assessment and damage alarm of bridge expansion joints using long-term structural health monitoring data", *Eng. Struct.*, **212**, 110520. https://doi.org/10.1016/j.engstruct.2020.110520

Pan, Q., Bao, Y. and Li, H. (2023), "Transfer learning-based data anomaly detection for structural health monitoring", *Struct. Health Monitor.*, **22**(5), 3077-3091. https://doi.org/10.1177/14759217221142174

Shi, C., Li, Y., Jiang, X., Sun, W., Zhu, C., Mo, Y., Yan, S. and Zhang, C. (2024), "Real-Time ConvNext-Based U-Net with Feature Infusion for Egg Microcrack Detection", *Agriculture*, **14**(9), 1655. https://doi.org/10.3390/agriculture14091655

Soleimani-Babakamali, M.H., Sepasdar, R., Nasrollahzadeh, K., Lourentzou, I. and Sarlo, R. (2022), "Toward a general unsupervised novelty detection framework in structural health monitoring", *Comput.-Aided Civil Infrastr. Eng.*, **37**(9), 1128-1145. https://doi.org/10.1111/mice.12812

Su, X., Mao, J., Wang, H., Gao, H. and Li, D. (2025), "Deep learning-based automated identification on vortex-induced vibration of long suspenders for the suspension bridge", *Mech. Syst. Signal Process.*, **224**, 112070. https://doi.org/10.1016/j.ymssp.2024.112070

Sun, L., Shang, Z., Xia, Y., Bhowmick, S. and Nagarajaiah, S. (2020), "Review of bridge structural health monitoring aided by big data and artificial intelligence: From condition assessment to damage detection", *J. Struct. Eng.*, **146**(5), 04020073. https://doi.org/10.1061/(ASCE)ST.1943-541X.0002535

Tahir, H., Khan, M.S. and Tariq, M.O. (2021), "Performance analysis and comparison of faster R-CNN, mask R-CNN and ResNet50 for the detection and counting of vehicles", *2021 International Conference on Computing, Communication, and Intelligent Systems (ICCCIS)*, Greater Noida, India, pp. 587-594. https://doi.org/10.1109/ICCCIS51004.2021.9397079

Wang, H., Tao, T., Li, A. and Zhang, Y. (2016), "Structural health monitoring system for Sutong cable-stayed bridge", *Smart Struct. Syst., Int. J.*, **18**(2), 317-334. https://doi.org/10.12989/sss.2016.18.2.317

Wang, Y., Huang, R., Song, S., Huang, Z. and Huang, G. (2021), "Not all images are worth 16x16 words: Dynamic transformers for efficient image recognition", *Adv. Neural Inform. Process. Syst.*, **34**, 11960-11973.

Weiss, K., Khoshgoftaar, T.M. and Wang, D. (2016), "A survey of transfer learning", *J. Big Data*, **3**(1), 1-40.

https://doi.org/10.1186/s40537-016-0043-6
Wen, L., Li, X. and Gao, L. (2020), "A transfer convolutional neural network for fault diagnosis based on ResNet-50", *Neural Comput*. *Applicat*., **32**, 6111-6124. https://doi.org/10.1007/s00521-019-04097-w
Wong, K.Y. (2007), "Design of a structural health monitoring system for long-span bridges", *Struct*. *Infrastr*. *Eng*., **3**(2), 169-185. https://doi.org/10.1080/15732470600591117
Xu, Z., Wang, H., Zhao, K., Zhang, H., Liu, Y. and Lin, Y. (2024), "Evolutionary probability density reconstruction of stochastic dynamic responses based on physics-aided deep learning", *Reliabil*. *Eng*. *Syst*. *Safety*, **246**, 110081. https://doi.org/10.1016/j.ress.2024.110081
Yarnold, M.T. and Moon, F.L. (2015), "Temperature-based structural health monitoring baseline for long-span bridges", *Eng*. *Struct*., **86**, 157-167. https://doi.org/10.1016/j.engstruct.2014.12.042
Ye, X.J., Wu, P., Liu, A., Zhan, X., Wang, Z. and Zhao, Y. (2023), "A deep learning-based method for automatic abnormal data detection: Case study for bridge structural health monitoring", *Int*. *J*. *Struct*. *Stabil*. *Dyn*., **23**(11), 2350131. https://doi.org/10.1142/S0219455423501316.
Zhang, Y. and Yuen, K.V. (2021), "Crack detection using fusion features-based broad learning system and image processing", *Comput*.*-Aided Civil Infrastr*. *Eng*., **36**(12), 1568-1584. https://doi.org/10.1111/mice.12753
Zhang, Y. and Yuen, K.V. (2022), "Review of artificial intelligence-based bridge damage detection", *Adv*. *Mech*. *Eng*., **14**(9), 1-21. https://doi.org/10.1177/16878132221122770
Zhang, Y.M., Wang, H., Bai, Y., Mao, J.X. and Xu, Y.C. (2022), "Bayesian dynamic regression for reconstructing missing data in structural health monitoring", *Struct*. *Health Monitor*., **21**(5), 2097-2115. https://doi.org/10.1177/14759217211053779
Zhou, G.D., Yi, T.H., Li, W.J., Zhong, J.W. and Zhang, G.H. (2020), "Standardization construction and development trend of bridge health monitoring systems in China", *Adv*. *Bridge Eng*., **1**(1), 1-18. https://doi.org/10.1186/s43251-020-00016-5
Zhuang, F., Qi, Z., Duan, K., Xi, D., Zhu, Y., Zhu, H., Xiong, H. and He, Q. (2020), "A comprehensive survey on transfer learning", *Proceedings of the IEEE*, **109**(1), 43-76. https://doi.org/10.1109/JPROC.2020.3004555